

**EXTRATROPICAL CYCLONES IN THE SOUTHERN HEMISPHERE:
COMPARISON AMONG DIFFERENT REANALYSES**

MARRAFON, Vitor Hugo - vitorhmarrafon@gmail.com
Universidade Federal de Itajubá / UNIFEI

REBOITA, Michelle Simões - reboita@unifei.edu.br
Universidade Federal de Itajubá / UNIFEI

DA ROCHA, Rosmeri Porfírio – rosmerir@model.iag.usp.br
Universidade de São Paulo / USP

CRESPO, Natália Machado – nataliacrespo@alumni.usp.br
Universidade de São Paulo / USP

Submetido em: 11/06/2020

Aceito para publicação em: 04/01/2021

Publicado em: 06/04/2021

DOI: <http://dx.doi.org/10.5380/abclima.v28i0.74460>

ABSTRACT: Extratropical cyclones are systems responsible for weather and climate changes. The knowledge of their main features is obtained by extensive databases and algorithms. There are several studies for the Northern Hemisphere (NH) that compare the climatology of cyclones in different reanalyses, whereas for the Southern Hemisphere (SH) there are few studies with this focus. In that sense, the objective of this study is to evaluate and compare cyclones climatology in different reanalyses for the SH. Here, cyclones at the south of 20°S are identified through the mean sea level pressure field in six reanalyses (NCEP1, NCEP2, NCEP20C, ERAI, ERA5 and ERA20C) using an automatic scheme. There are two periods under analysis: a long one (1900-2010), which includes the centennial reanalyses (NCEP20C and ERA20C), and a short one (1980-2018), which includes the four other reanalyses. Regarding the centennial reanalyses, the NCEP20C shows a positive and statistically significant trend of the cyclone frequency, while the ERA20C indicates a negative trend of these systems. Comparing the six reanalyses, those with higher resolution are the ones that register the largest number of cyclones, but this does not affect the climatological characteristics of the cyclones, such as the annual cycle pattern, which is similar in all datasets. The trend of intense cyclones (reaching a central pressure lower than 980 hPa) shows an increase in all reanalyses. An interesting result of the centennial reanalyses is that the trend of all cyclones in the SH decreases in mid-latitudes and increases around Antarctica, which is a signal similar to that of the climate projections.

KEYWORDS: extratropical cyclones, trend, Southern Hemisphere, South Atlantic Ocean

CICLONES EXTRATROPICAIS NO HEMISFÉRIO SUL: COMPARAÇÃO ENTRE DIFERENTES REANÁLISES

RESUMO: Os ciclones extratropicais são sistemas responsáveis por mudanças no tempo e clima das regiões onde atuam. O conhecimento de suas características médias é obtido por meio de extensas bases de dados e códigos computacionais. Há vários estudos para o Hemisfério Norte (HN) que comparam a climatologia dos ciclones em diferentes reanálises. Como para o Hemisfério Sul (HS) há poucos estudos com esse enfoque, esse é o objetivo do presente trabalho. Aqui, os ciclones ao sul de 20°S são identificados no campo da pressão atmosférica ao nível médio do mar em seis reanálises (NCEP1, NCEP2, NCEP20C, ERAI, ERA5 e ERA20C) e com um esquema automático. Dois períodos são analisados: um longo (1900-2010), que inclui as reanálises centenárias (NCEP20C e ERA20C), e um curto (1980-2018), que engloba as outras quatro reanálises. Com relação

às reanálises centenárias, para todo o HS, o NCEP20C mostra tendência positiva e estatisticamente significativa da frequência de ciclones, enquanto a ERA20C indica tendência negativa. Comparando as seis reanálises, aquelas com maior resolução são as que fornecem o maior número de ciclones, o que não afeta as características climatológicas dos ciclones, como o padrão do ciclo anual, por exemplo, que é similar em todos os conjuntos. A frequência de ciclones intensos (que atingem pressão central menor do que 980 hPa) mostra tendência de aumento em todas as reanálises. Um resultado interessante nas reanálises centenárias é que a tendência de todos os ciclones no HS diminui em latitudes médias e aumenta ao redor da Antártica, sinal similar ao das projeções climáticas.

PALAVRAS-CHAVE: ciclones extratropicais, tendência, Hemisfério Sul, oceano Atlântico Sul

1. INTRODUCTION

Cyclones, regardless of type (extratropical, subtropical or tropical), are of great interest to the scientific community and the population because they cause weather and climate changes. Extratropical cyclones are those formed outside tropical regions and are associated with the presence of horizontal gradients of surface air temperature and the influence of waves on the flow in medium/high levels of the atmosphere (Celemín, 1984; Reboita et al., 2017). The study of climatological characteristics (genesis regions, displacement, lifetime etc.) of extratropical cyclones throughout the 20th century is an important way to understand trends in the precipitation (Kunkel et al., 2012) and winds (Vessey et al., 2020) extremes.

Extratropical cyclones can be studied using reanalysis data, which is a combination of observed and modeled data. As there are different methods of data assimilation and different configurations of the atmospheric models and horizontal resolution used in these models, the reanalysis sets differ from each other, which may cause uncertainties in the results of cyclonic activity (Hodges et al., 2008, 2011; Allen et al., 2010). Therefore, studies have been carried out in order to compare the climatological characteristics of cyclones in different reanalyses (Table 1). For example, Befort et al. (2016) found differences in the cyclones trend in the NCEP-20C and ERA-20C reanalyses in both Southern (SH) and Northern (NH) Hemispheres. Tilinina et al. (2013) analyzed the extratropical cyclones trend in NH recorded in five reanalyses, and only the National Center for Environmental Prediction Reanalysis 1 (NCEP1) and ERA-Interim (ERA-Interim; from the European Centre for Medium-Range Weather Forecasts) had a positive and significant linear trend, from 1 to 2% per decade, in the total number of cyclones. Chang and Yau (2016) compared the cyclonic activity of five reanalyses with that of radiosonde data in the NH. While the reanalyses showed an increase in the trend, the radiosonde data indicated a decrease in the cyclones frequency. Reboita et al. (2015) showed that the trend of all cyclones identified in the NCEP1 reanalysis for the SH is increasing, influenced by the greater number of intense cyclones since the weaker ones are less frequent. Reboita et al. (2018) compared the frequency of cyclones in the South Atlantic Ocean in five reanalyses (NCEP1, NCEP2, ERA-40, ERA-Interim and CFSR) and found that CFSR reanalysis was the one that registered the highest frequency of cyclones, while NCEP1 and NCEP2, the lowest occurrence of these systems. This fact can be explained by the higher spatial resolution of the model that generates the CFSR reanalysis, which better solves the cyclonic circulation centers. A similar study was carried out by Crespo et al. (2020a), who compared

the climatology of three reanalyses (ERA5, ERAI and CFSR), using the same tracking algorithm as Reboita et al. (2018). The authors found that CFSR has the highest number of cyclones, while ERAI the lowest. de Jesus et al. (2020), through an ensemble of ERAI and CFSR reanalyses, found a negative trend in the frequency of cyclones in the period 1979 to 2005, which is in agreement with Reboita et al. (2015) for the time slice 1980 to 2000.

In addition to the uncertainties arising from the data source, cyclone climatology may also have uncertainties associated with the atmospheric variable used to identify these systems, as well as with the algorithm used (Leonard et al., 1999; Neu et al., 2013). For example, Vessey et al. (2020) found fewer cyclones in the Arctic using MSLP rather than vorticity, and this difference reaches almost 50% from December to February. Crespo (2019), comparing two cyclone climatologies using ERAI for the period 1979 to 2017, one obtained with MSLP data and the other with the relative vorticity of the wind at 925 hPa, found that the cyclogenetic density obtained with the two variables is similar in subtropical regions, over the continent and close to the coast. However, at mid-latitudes, there is a higher frequency of cyclones when using relative vorticity. In addition, the systems appear slightly displaced to the southwest compared to those identified on the MSLP.

Table 1 summarizes several studies published from 2010 to the present day; it is observed that there are more studies comparing the climatology of cyclones in different reanalyses for the NH than for the SH. In the SH, studies for the South Atlantic are not so scarce but generally use only one data set. Therefore, this study aims to determine the climatology of extratropical cyclones in the SH in six reanalyses and to evaluate the cyclone frequency trend sign.

Table 1- Summary of studies from 2010 to the present day using different reanalyses to identify cyclones and their trends in different parts of the globe. In the table, SH stands for Southern Hemisphere; NH for Northern Hemisphere; MSLP for mean sea level pressure; and Vort for Vorticity.

Reference	Reanalyses	Period	Variable used to identify cyclones	Study area	Type of climatology (all cyclones or only the intense ones)	Reanalysis with more and less cyclones	Cyclone frequency trend
Allen et al. (2010)	ERA40, ERAI, NCEP2, JRA25	1979-2008	MSLP	SH and NH	Deep	+ERAI -NCEP2	+ ERAI, ERA40, NCEP2 and JRA-25
Hodges et al. (2011)	ERA1, JRA25, CFSR, MERRA	11979-2009 DDJF: NH JJA: SH	MSLP and Vort	SH and NH	All and intense	Merra produces a higher number of pressure-intensive cyclones than the CFSR as to vorticity	Not shown
Wang et al. (2013)	NCEP1, NCEP20C	1951-2010	MSLP	SH and NH	All	+NCEP1 -NCEP20C	+ NCEP1 and NCEP20C
Tilinina et al. (2013)	NCEP2, JRA25, ERAI, MERRA, CFSR	1979-2010	MSLP	NH	Total	+ MERRA - NCEP2	+ NCEP2 and ERAI
					Intense	+ MERRA - NCEP2	All show a negative trend in the last decade of the study
Tilinina et al. (2014)	ERA1, MERRA, CFSR, ASR	2000-2010	MSLP	Arctic	All	+ ASR	No trend
					Intense	+ASR	Negative
Reboita et al. (2015)	NCEP1	1980-2012	MSLP	SH	All		Positive
					Intense		Positive
					Weak		Negative
Chang e Yau (2016)	NCEP2, ERA40, JRA55, NCEP20C, ERA20C	DJF 1959-2010	MSLP	NH	All	- NCEP20C	Positive in all, except in observed radiosonde data
Wang et al. 2016	ERA20C, NCEP20C, JRA55, MERRA, CFSR, ERAI, ERA40, NCEPI, NCEP2	1979-2001	MSLP	SH and NH	All	+ MERRA - NCEP20C	In general, data from 1958 to 2010 show a positive trend in both hemispheres
Befort et al. (2016)	NCEP20C, ERA20C	1901-2008	MSLP	SH and NH	All	+ ERA20C and there is a substantial difference between	NH: + ERA20C and - NCEP20C SH: + ERA20C

						1931-1960	
Grieger et al. (2018)	ERA1	1979-2008	MSLP, Vort and geopotential height	Subantarctic region	All		Positive
Reboita et al. (2018)	CFSR, ERA1, ERA40, NCEP1, NCEP2	1979-2005	Vort	South Atlantic	All	+ CFSR - NCEP1 and NCEP2	Not shown
Zahn et al. (2018)	ERA1, MERRA2, CFSR, JRA25	1981-2010	MSLP	Arctic	All		ERA1 and Merra + in DJFCFSR and JRA55 -
					Intense	Similar in all sets	Only JRA55 -
Bloomfield et al. (2018)	ERA20C, ERA1, ensemble CERA20C and ERA20C	1900 - 2010	Vort	NH	All		Not shown
Wickström et al. (2019)	ERA1	DJF: 1979-2016	MSLP	North Atlantic	Intense		+ERA1
Kayano et al. (2019)	NCEP2	1970-2017	Vort	South Pacific and South Atlantic	Intense		Negative
Crespo (2019)	ERA1	1979-2017	MSLP and Vort	SH	All		Not shown
Crespo et al. (2020a)	ERA1, ERA5, CFSR	1979-2018	Vort	South Atlantic	All	+CFSR - ERA1	Not shown
de Jesus et al. (2020)	Ensemble CFSR and ERA1	1979-2005	Vort	South Atlantic	All		All period, a negative trend; from 1989 to 2005, a positive trend
Vessey et al. (2020)	ERA1, JRA55, MERRA2, CFSR	1980-2017	MSLP and Vort	Arctic	All	Similar in all sets. The number of cyclones is greater when identified with vorticity.	No significant trend

2. METHODOLOGY

2.1 DATA

In this study, MSLP data are used every six hours in six reanalyses: three from the National Center for Environmental Prediction-NCEP (NCEP1, NCEP2 and NCEP20C) and three others from the European Center for Medium-Range Weather Forecasts - ECMWF (ERA1, ERA5 and ERA20C), as shown in Table 2. These reanalyses differ in spatial resolution as well as in the methods of data assimilation and the configurations of the models that produce them.

The study covers two periods according to the available data: a long one (1900-2010), which includes the centennial reanalyses NCEP20C and ERA20C, and a short one (1980-2018), including the four other reanalyses.

Before using the algorithm for the cyclones identification and tracking, all reanalyses were interpolated to the same grid with a resolution of 2.5° following Kodama et al. (2019). This operation smooths the MSLP field and avoids identifying noises as a cyclone when using high resolution data (such as ERA5), which are called spurious or unrealistic cyclones (Sinclair, 1994).

Table 2 Characteristics of the reanalyses used in the study.

Reanalyses	Resolution	Period	Reference
NCEP1	2.5° x 2.5°	1980 - 2018	https://www.esrl.noaa.gov/psd/data/gridded/data.ncep.reanalysis.html (Kalnay et al., 1996)
NCEP2	2.5° x 2.5°	1980 - 2018	https://www.cpc.ncep.noaa.gov/products/wesley/reanalysis2/kana/reanl2-1.htm (Kanamitsu et al., 2002)
NCEP20C	2.0° x 2.0°	1900 - 2010	https://www.esrl.noaa.gov/psd/data/20thC_Rean/ (Compo et al., 2011)
ERA-Interim	0.75° x 0.75°	1980 - 2018	https://apps.ecmwf.int/datasets/data/interim-full-daily/levtype=sfc/ (Berrisford et al., 2011).
ERA5	0.25° x 0.25°	1980 - 2018	https://cds.climate.copernicus.eu/#!/search?text=ERA5&type=dataset (Hersbach et al., 2019)
ERA20C	1.25° x 1.25°	1900 - 2010	https://apps.ecmwf.int/datasets/data/era20c-daily/levtype=sfc/type=an/ (Poli et al., 2016)

2.2 CYCLONE IDENTIFICATION AND TRACKING ALGORITHM

The scheme used to identify and track cyclones in this study is that of Murray and Simmonds (1991a, b), developed at the University of Melbourne, Australia. This algorithm was part of a project that involved the intercomparison of 15 extratropical cyclone identification algorithms (Neu et al., 2013), called Intercomparison of Mid Latitude Storm Diagnostics (IMILAST). It has also recently been used to track cyclones in the subantarctic region (Grieger et al., 2018). In addition, the Murray and Simmonds algorithm has been used since 2004 by the Climate Studies Group from the University of São Paulo (GrEC-USP; www.grec.iag.usp.br) and shows a good performance in the identification of extratropical cyclones in the SH (Pezza and Ambrizzi, 2003; Reboita et al.,

2015) and in other regions of the globe (Leckebusch and Ulbrich, 2004; Pinto et al., 2005; Leckebusch et al., 2006; Kruschke et al., 2014; Befort et al., 2016).

MSLP at every six hours is the input data for the algorithm. The literature has shown a discussion as to whether vorticity or MSLP is the most appropriate variable for identifying cyclones. There is not a single answer to this question, since both variables have positive and negative qualities (details on this subject are presented in Reboita, 2008). The IMILAST project, for example, includes algorithms based on both pressure and vorticity and a general result is that the algorithms using vorticity detect a higher frequency of cyclones in comparison with that based on MSLP (Neu et al., 2013).

Initially, the algorithm interpolates the MSLP from regular to polar-stereographic, centered on the SH, using the bicubic spline interpolation method. The routine for identifying low pressure centers starts by looking for an array (set of grid points) with the maximum Laplacian pressure value. The position of the minimum pressure is then located by an interactive approach to the center of the ellipsoid with a better representation of surface pressure, which is also done through bi-cubic splines. The pressure Laplacian is considered a measure of the system intensity. In order to exclude weak systems, low pressure centers that do not reach a minimum value pre-specified for the pressure Laplacian are avoided (Simmonds et al., 1999). As the pressure Laplacian is proportional to the cyclonic relative geostrophic vorticity, this method ends up approaching the algorithms based on relative vorticity to identify cyclones, such as the one used by Sinclair (1994) and Reboita et al. (2010, 2018).

The cyclone tracking procedure involves three stages: (a) the subsequent position of a low pressure center is initially predicted, (b) the identification probability between the projected cyclone and each low center present in the new synoptic schedule is calculated and (c) the combination of the position of a cyclone at a given time (t) and the next time ($t + dt$) is based on the highest probability of association between the centers identified in two consecutive times (further details on the method are presented in Simmonds et al., 1999, 2003).

The Murray and Simmonds scheme has a large number of parameters that must be set by the user. Here, the configurations proposed by Pezza and Ambrizzi (2003) and by Reboita et al. (2015) are used. These settings include, for example, the "iopmxc" parameter, which, if set to zero, only indicates the inclusion of low-pressure systems with closed isobars; and the "mscrn" parameter, which represents the tracking method and, when set to 2, corresponds to the maximum Laplacian.

The algorithm provides the trajectory of each cyclone (latitude and longitude) throughout the lifecycle, as well as statistical data regarding the trajectory density (SD), central pressure (PC), intensity, radius (R) and depth (D) of cyclones. The SD corresponds to the normalized number of systems that pass by a given area. The measurement of the cyclone intensity is provided by the Laplacian pressure field (calculated between the center of the system and the neighborhood) and, according to Simmonds and Murray (1999), must exceed $0.2 \text{ hPa (lat)}^{-2}$ to be considered. D is the difference (in pressure) between the system center and the region where the Laplacian turns zero (which associates the cyclone outermost isobar), and R is the distance between

these two points (Lim and Simmonds, 2007). All statistics are presented in a grid with a horizontal resolution of 2.5°.

For the climatology, only cyclones that have a lifespan of 24 hours or more and were formed south of 20°S are included (this avoids the inclusion of tropical systems). Cyclone frequency is defined as the number of systems per month, season (DJF, MAM, JJA and SON) and year.

2.3 ANALYSES

The study presents the climatologies of the cyclone frequency in the SH and for the South Atlantic Ocean (defined by the region between 80°W-20°E and 90°-20°S), once many extratropical cyclones are formed in this region, impacting the South American east coast. Statistics are calculated for all cyclones with a lifespan of 24 hours or more and for the intense systems, that is, systems that have central pressure equal or lower than 980 hPa at some point in its life cycle (Tilinina et al., 2013, 2014; Reboita et al., 2015). In addition, the seasonal average of the cyclogenesis density, the cyclone trajectory density and the central pressure of all systems are presented for the SH. As the cyclogenesis density (initial cyclones position) is not provided by the algorithm, this is calculated considering the area of 2.5°x2.5° and normalized by the same area.

The trend of cyclone frequency is obtained using the linear regression method calculated from the least-squares. The Mann-Kendall non-parametric test of statistical significance (Kendall, 1938) is used as an indicator of the statistical significance of the trend at the confidence level of 95%. All analyses described here are performed for the six reanalyses defined in Table 2.

3. RESULTS

3.1 ANNUAL FREQUENCY AND TRENDS

The annual frequency of extratropical cyclones considering all cyclones identified by the algorithm (Figure 1) and those with pressure lower than or equal to 980 hPa ($P \leq 980$ hPa) at some point in their lifecycle (Figure 2) is presented for the entire SH and in the South Atlantic Ocean. For the SH and all cyclones (Figure 1a), regarding the centennial reanalyses (NCEP20C and ERA20C), NCEP20C shows a steep and statistically significant positive trend while ERA20C presents a significant negative trend. The trend sign and indication of those that are statistically significant at the 95% confidence level are shown in Table 3. For the recent reanalyses, all data sets show a positive trend that is not significant only in ERA5. For the intense systems in the SH (Figure 2a), both centennial reanalyses indicate a positive and statistically significant trend. These results agree with several of the studies compiled in Table 1, such as Allen et al. (2010), who showed a positive trend in the frequency of strong cyclones in ERAI and NCEP2; Reboita et al. (2015), who showed this same result using NCEP1; and Wang et al. (2016) and Grieger et al. (2018), who obtained a positive trend considering all cyclones registered in NCEP20C and ERAI, respectively.

For all cyclones over the South Atlantic Ocean (Figure 1b), ERA20C shows a negative trend in the frequency of the system, while NCEP20C shows a positive one, which agrees with the hemispheric analysis. Regarding intense systems (Figure 2b) in the South Atlantic, all six reanalyses indicate a positive trend, but with ERAI and ERA5 not showing any statistically significant trend (Table 3).

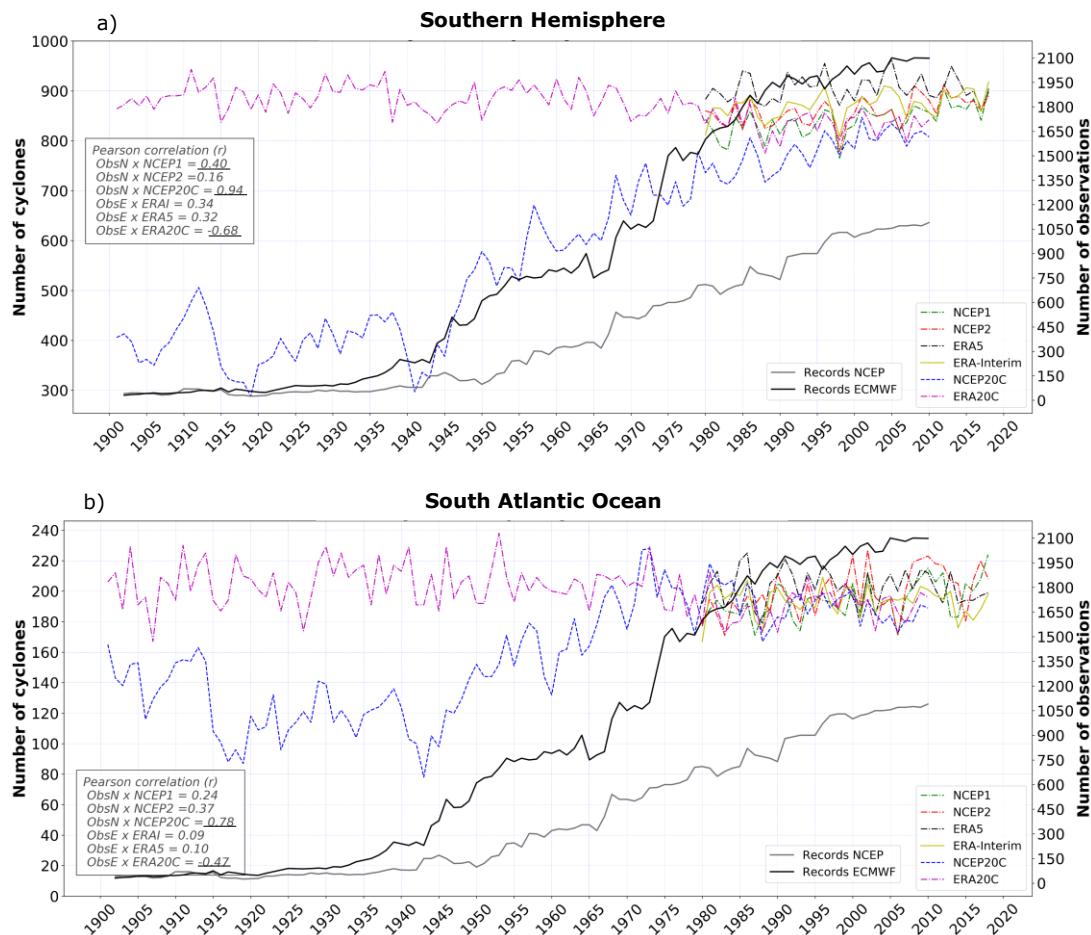


Figure 1 - Annual frequency of all extratropical cyclones considering the different reanalyses: (a) Southern Hemisphere and (b) South Atlantic Ocean. The gray and black lines indicate the number of surface observations assimilated in the NCEP (Compo et al., 2011) and in the ECMWF (Poli et al., 2016) reanalyses, respectively. The correlation between the number of surface observations assimilated in the reanalyses (ObsN for NCEP and ObsE for ECMWF) and the cyclones frequency are shown in the frame inside the figure, where the significant correlations at the 95% confidence level are underlined.

Table 3 - Trend (inclination angle) of the annual frequency series of extratropical cyclones. A positive (negative) value indicates a positive (negative) trend. Values with statistical significance at the 95% level are highlighted in bold.

Reanalyses	All cyclones		Cyclones with P ≤ 980 hPa	
	Southern Hemisphere	South Atlantic	Southern Hemisphere	South Atlantic
NCEP1	1.53	0.56	1.60	0.46
NCEP2	1.10	0.75	1.44	0.58
ERA5	0.23	-0.13	0.67	0.04
ERA-Interim	1.10	-0.10	0.97	0.12
NCEP20C	5.21	0.87	4.22	0.63
ERA20C	-0.59	-0.17	1.11	0.23

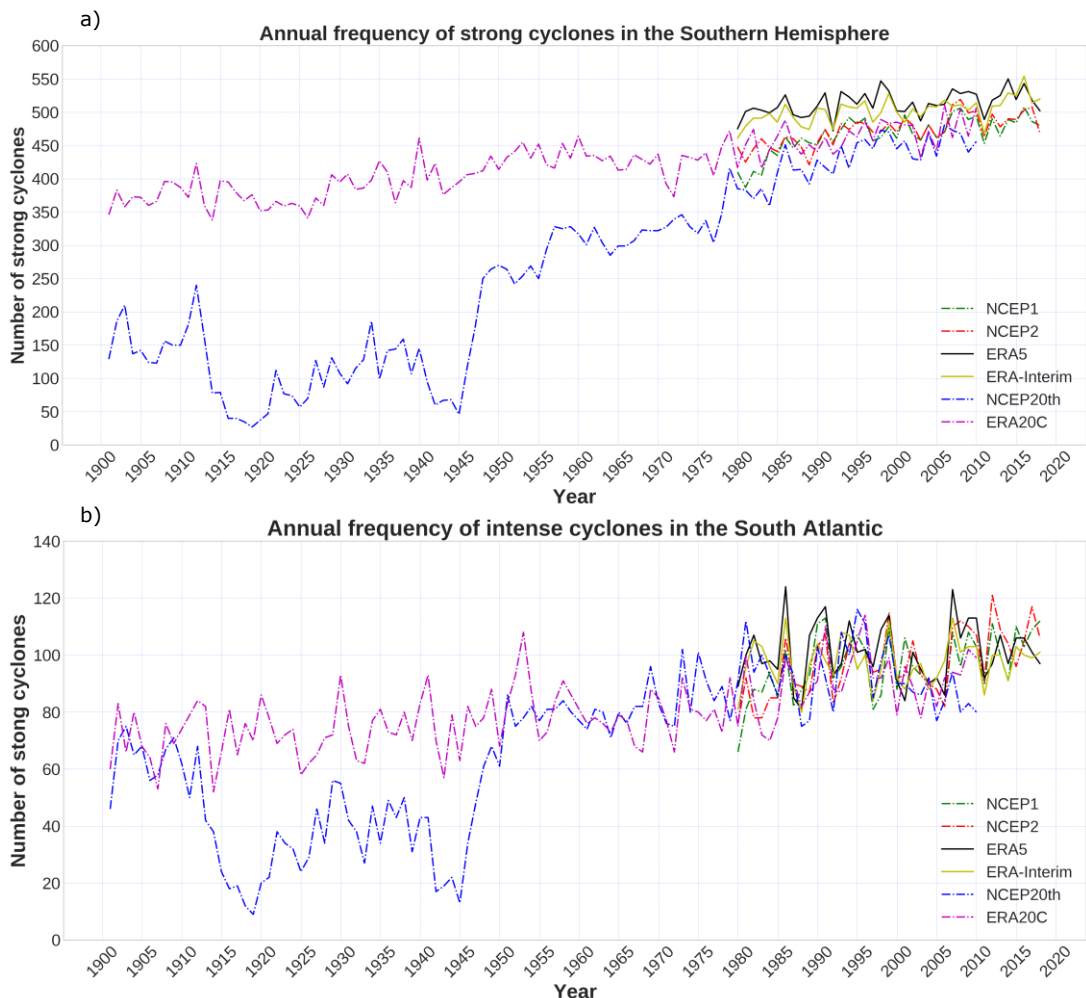


Figure 2 - Annual frequency of intense cyclones in the different reanalyses: (a) Southern Hemisphere and (b) South Atlantic Ocean.

The main information obtained from Figures 1 and 2 are: (a) all data sets agree that the number of intense cyclones has been increasing over the years. In the SH, the number of intense cyclones in the current reanalyses has

increased between 6 (ERA5) to 16 (NCEP1) cyclones per decade; (b) the reanalyses with a higher horizontal resolution register a higher number of cyclones, which is shown by the higher cyclones frequency in ERA5, followed by ERAI and those from NCEP; and (c) there is a great difference in the cyclones frequency recorded in the centennial reanalyses (ERA20C and NCEP20C).

Regarding item (b), even if all reanalyses have been interpolated to the same horizontal resolution, they preserve their original information; hence, those obtained by numerical models with a higher horizontal resolution can resolve a greater number of cyclones (Tilinina et al., 2013; Hodges et al., 2017; Reboita et al., 2018).

To elucidate the difference in the cyclones frequency between the centennial reanalyses (item c), we addressed three points: (1) the relationship between the number of surface observations assimilated over the years in the numerical models for the generation of these reanalyses and the cyclones frequency, (2) the values of the MSLP in the reanalysis and (3) the impact of some teleconnection patterns on the cyclones climatology.

Assimilated surface observations: We begin evaluating the relationship between the number of surface observations assimilated over the years in the numerical models for the generation of these reanalyses and the cyclones frequency. The number of observations by year in each reanalysis was obtained by converting Figure 3b from Compo et al. (2011) and Figure 1a from Poli et al. (2016) in time series. From the time series of the number of assimilated observations along with the annual cyclones frequency (Figure 1), it is noted that there is a positive linear trend in the number of observations assimilated in both NCEP20C and ERA20C, but with higher number of information assimilated in ERA20C compared to the NCEP20C from 1940. While the increase in the annual cyclones frequency in NCEP20C seems to be a function of the increase in assimilated observations, this result is different in ERA20C, where there is a slight decrease in the cyclones frequency. Therefore, it is suggested that the numerical model used in the generation of the NCEP20C reanalysis is more sensitive to the assimilated data than that of the ERA20C. The result obtained here also agrees with Wang et al. (2013), who mention that the NCEP20C reanalysis has no homogeneities in the number of cyclones and that this is associated with the change in the number of observed data used in the assimilation during the 20th century. Another fact is that ERA20C, different from NCEP20C, assimilates near-surface winds over the oceans, which is an important variable for the cyclone's identification, mainly in the SH where the oceans are predominant. In addition, there are differences in data assimilation schemes between reanalyses.

MSLP: A second point is the comparison in terms of MSLP average. The hypothesis here for the difference in the number of cyclones would be that the NCEP20C reanalysis had a higher atmospheric pressure in the first decades than the ERA20C. Thus, it could generate weaker cyclones and/or with shorter lifetime, not being detected by the algorithm. Figure 3 shows the comparison of the annual MSLP average considering the entire SH, and reveals that until 1955 both reanalyses have an annual average (1009.4 hPa for NCEP20C and 1008.7 hPa for ERA20C) slightly higher than that of the most recent period (1008 hPa for NCEP20C and 1007.6 for ERA20C), with the difference between the two periods about 1 hPa. Although MSLP in the NCEP20C is slightly higher than that

of ERA20C, this does not explain the difference in the cyclones frequency, since the difference is practically constant over the whole period (Figure 3).

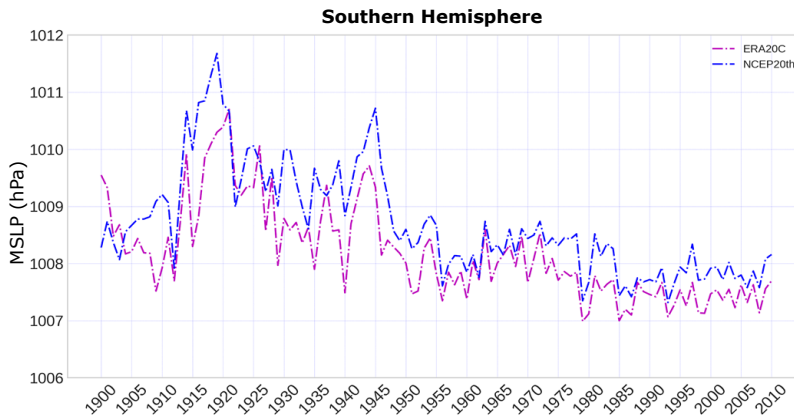


Figure 3 - MSLP annual average (hPa) for the entire Southern Hemisphere in the NCEP20C (blue line) and ERA20C (purple line) reanalyses.

Teleconnection Patterns: Figures 1a and 3 indicate that the time series change patterns from approximately 1955. This could suggest the influence of some low-frequency teleconnection patterns of the atmosphere in such configurations. In this context, a third approach is to relate the cyclones frequency anomalies with two specific low-frequency patterns.

Figure 4 shows the annual Pacific Decadal Oscillation Index (PDO; Mantua et al., 1997) along with the detrended time series of annual anomalies of cyclone frequency in NCEP20C and ERA20C. PDO is a climate variability pattern characterized by anomalies of opposite signs (sea surface temperature, atmospheric pressure etc.) between the tropical-northeastern and central-northwestern North Pacific Ocean. The hypothesis here is that periods of positive PDO phase (positive anomalies of sea surface temperature predominating in the eastern North Pacific, along with the North American coast, and central-eastern Tropical Pacific) may be favorable to the reduction of atmospheric pressure in southern latitudes and, consequently, favoring higher frequency of cyclones. From 1900 to 1955, the PDO changed from a positive to a negative phase and then to a positive one, showing no persistence in a single phase, in that sense, it does not justify the pattern of atmospheric pressure shown in Figure 3. After 1955, there is a preference for the negative phase of the PDO, which would be favorable to the increase in pressure (unfavorable to cyclones) and, therefore, indicating opposite results to those shown in Figure 3, in which there is a record of the lowest MSLP annual average. As shown through the visual analysis of Figure 4 and Pearson's correlation coefficient, there is no relationship between PDO and the cyclones frequency.

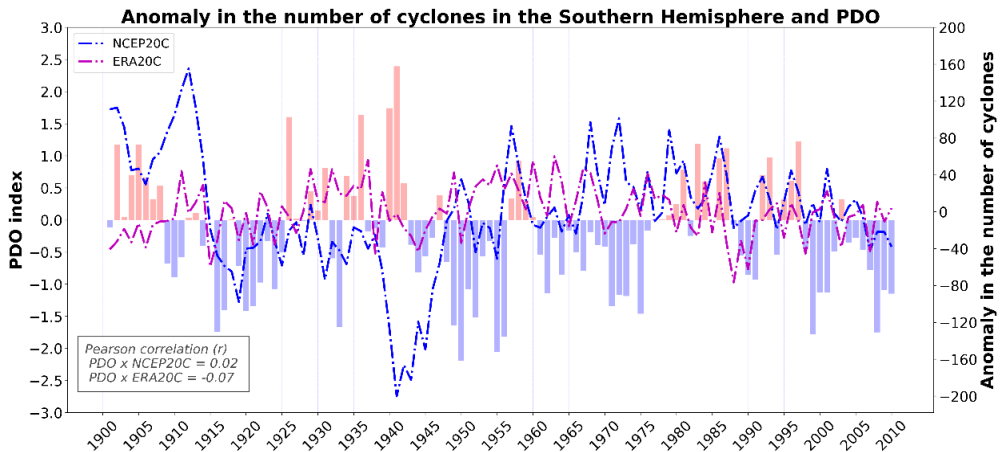


Figure 4 - Annual Pacific Decadal Oscillation Index (PDO; <https://www.ncdc.noaa.gov/teleconnections/pdo/>; bars) and the detrended time series of the anomaly of the extratropical cyclones frequency (1900-2010) in the SH (all systems) for NCEP20C (blue line) and ERA20C (purple line). The frame inside the figure indicates the correlation between the series of centennial reanalyses and the anomaly of cyclones frequency.

Another low-frequency variability pattern that may impact the cyclones occurrence is the Atlantic Multidecadal Oscillation (AMO; Kayano et al., 2019), characterized by sea surface temperature anomalies in the North Atlantic. The periods with cold (warm) anomalies correspond to the AMO cold (warm) phase (Enfield et al., 2001) and can last for 20 to 40 years (https://www.aoml.noaa.gov/phod/amo_faq.php). Kayano et al. (2019) showed that AMO had a negative phase between 1979-1993 (which coincided with the PDO positive phase) and a positive one between 2003-2017 (coinciding with a PDO oscillation from positive - 2003-2006 - to negative - 2014-2017). These phases are evident in Figure 5a, which begins in 1948, the year when the AMO index was made available by NOAA. The final year (2010) in the figure is the last year available in centennial reanalyses.

Figure 5a shows the AMO annual index along with the time series of anomalies of the cyclones annual frequency (detrended) in the SH for the centennial reanalyses. The NCEP20C reanalysis clearly shows a pattern opposite to that of AMO, with positive (negative) cyclone anomalies in periods of cold (warm) AMO phases, giving a correlation coefficient of -0.47 (with 95% confidence statistical significance). On the other hand, the inverse relationship occurs between ERA20C and AMO in shorter periods compared to the results of NCEP20C. For example, between 1973 and 1979 there are positive anomalies in the cyclones occurrence in ERA20C concomitantly with the cold AMO phase. The same analysis is performed considering only the period from 1980 to 2018 for all cyclones identified in the SH (Figure 5b) and only in the South Atlantic (Figure 5c) in the NCEP1, NCEP2, ERAI and ERA5 reanalyses. In general, there is a negative correlation between the time series of cyclones occurrence and AMO, with the highest correlations (although without statistical significance) in the ECMWF reanalyses (Figure 5b-c).

The results from Figure 5 are in agreement with those of Kayano et al. (2019), who analyzed the cyclones relationship in the region between the Southeast Pacific and the South Atlantic oceans from 1979 to 2017, considering

the NCEP2 reanalysis and the summer and winter seasons. The authors obtained a higher (lower) cyclones frequency in both oceans and seasons in the cold (warm) AMO phase. Kayano et al. (2019) associated their results with the distinct patterns of sea surface temperature anomalies in the SH in both AMO phases. For example, in the negative (positive) AMO phase at high and middle latitudes, there are positive (negative) temperature anomalies on the sea surface. In short, even if the cyclone frequency has a response to AMO, it also does not explain the difference in trends between centennial reanalyses.

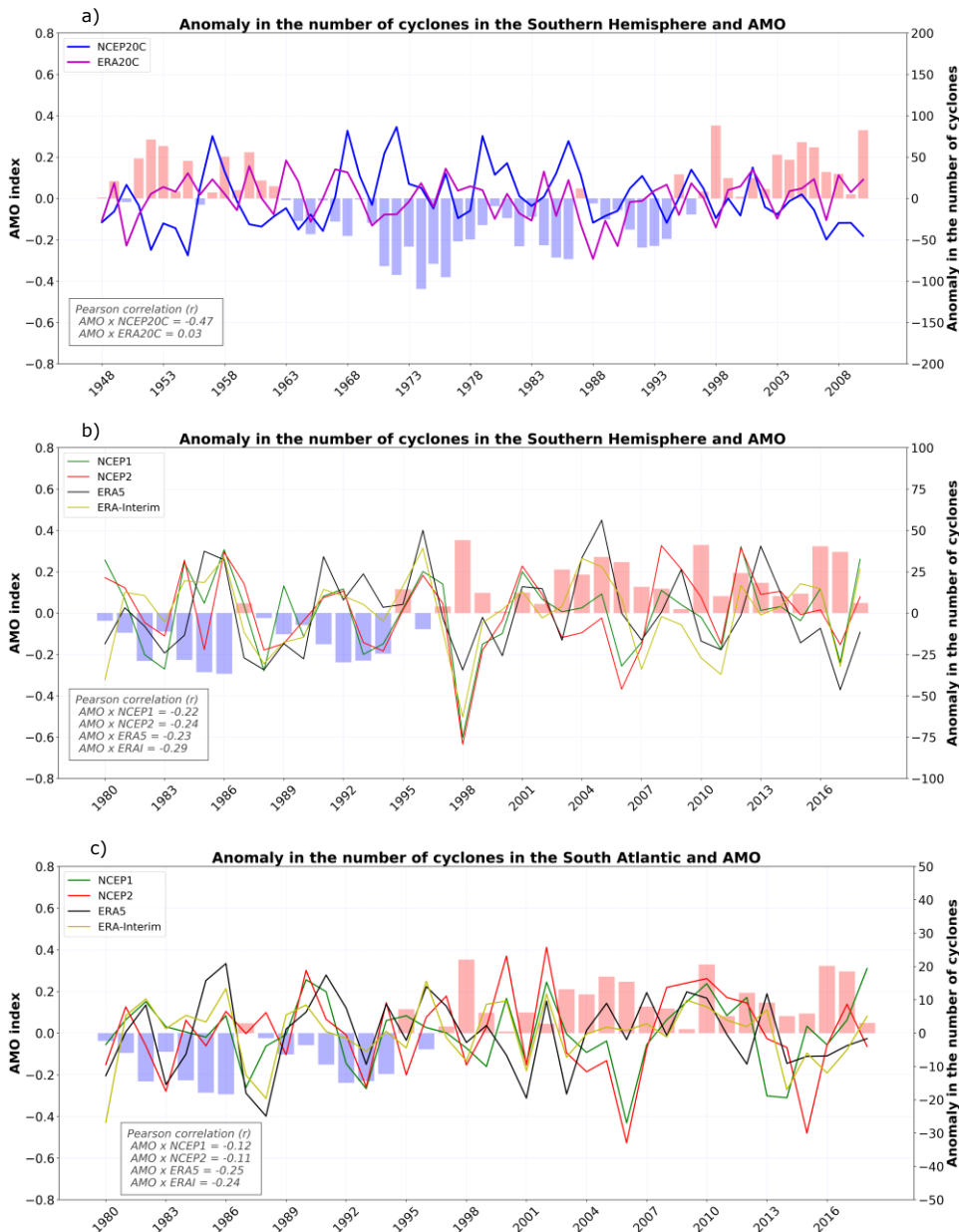


Figure 5 - Time series of the annual Atlantic Multidecadal Oscillation Index (AMO; <https://www.psl.noaa.gov/data/correlation/amon.us.data>; bars) and detrended time series of the anomaly of the extratropical cyclones frequency (all systems identified; lines). a) NCEP20C (blue line) and ERA20C (purple line) in the SH (1948 to 2010). The cyclone anomaly is regarding the climatology from 1900 to 2010; b) NCEP1, NCEP2, ERAI

and ERA5, considering the period from 1980 to 2018 in the SH; and c) NCEP1, NCEP2, ERAI and ERA5, considering the period from 1980 to 2018 in the South Atlantic. The frames inside each panel show the correlation between the annual time series of cyclone occurrence in each dataset and the AMO index. Only the correlation between NCEP20C and AMO has a statistical significance with 95% confidence.

3.2 SEASONALITY

The annual frequency cycle of all extratropical cyclones and those more intense in the SH is characterized by a higher occurrence in the winter and a lower one in the summer in all reanalyses (Figures 6a,c; Tables 4 and 5), except in NCEP20C for intense systems. This result agrees with several studies, such as Simmonds and Key (2000) and Reboita et al. (2015). When the analysis is restricted to the South Atlantic Ocean (Figures 6b, d), the highest cyclones frequency occurs in a very similar way between autumn and winter (Table 4) for all systems and the intense ones, a result that was also obtained by Reboita et al. (2010) in a specific study for the South Atlantic.

Regarding the data variability, the standard deviation is similar between reanalyses, except in NCEP20C, in which it presents the largest deviations in relation to the set average (Figure 6).

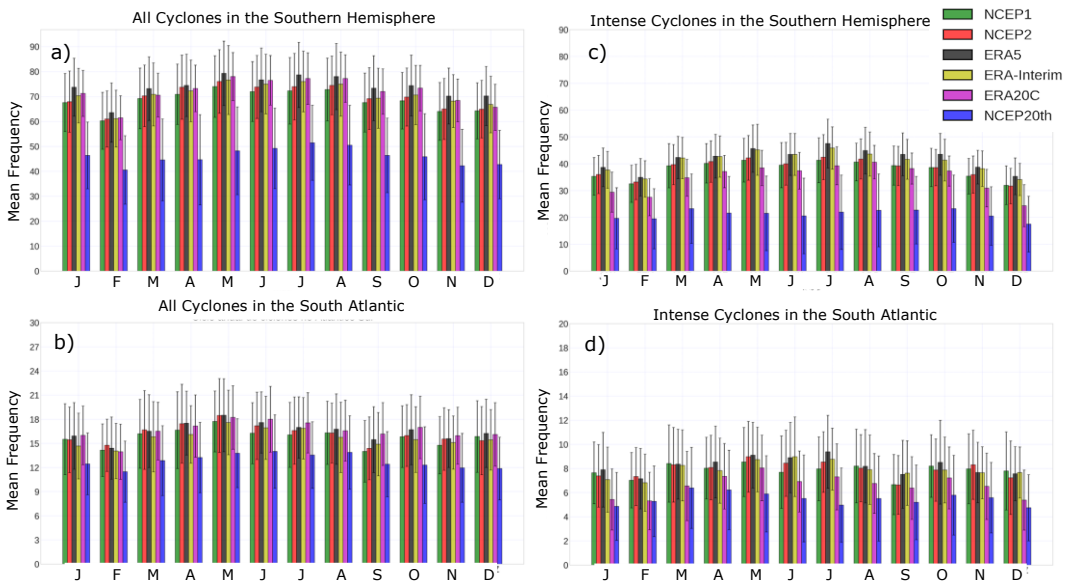


Figure 6- Annual frequency cycle of all cyclones identified by the algorithm (left column) and intense cyclones ($P \leq 980$ hPa) (right column) in the different reanalyses for the SH (a,c) and South Atlantic (b,d). The black lines at the top of each colored bar indicate the standard deviation.

Table 4 - Seasonal averaged frequency (absolute) of all cyclones identified in the SH and the South Atlantic.

Reanalyses	Southern Hemisphere				South Atlantic			
	DJF	MAM	JJA	SON	DJF	MAM	JJA	SON
NCEP1	64.0	71.3	72.3	66.7	15.2	16.8	16.2	14.9
NCEP2	64.5	73.3	74.0	67.9	15.2	17.5	16.9	15.3
ERA5	69.1	75.6	77.8	72.6	15.5	17.5	17.1	15.9
ERA1	66.1	73.2	75.3	69.3	14.7	16.5	16.5	15.1
NCEP20C	43.2	45.8	50.4	44.8	11.9	13.3	13.8	12.2
ERA20C	66.1	73.9	76.9	71.2	15.3	17.3	17.4	16.4

Table 5 - Seasonal averaged frequency (absolute) of cyclones that reach $P \leq 980$ hPa at some point in their lifecycle in the SH and the South Atlantic.

Reanalyses	Southern Hemisphere				South Atlantic			
	DJF	MAM	JJA	SON	DJF	MAM	JJA	SON
NCEP1	33.2	40.2	40.5	37.7	7.5	8.3	8.0	7.6
NCEP2	33.6	40.9	41.4	37.9	7.3	8.4	8.3	7.6
ERA5	36.3	43.6	45.3	41.9	7.5	8.6	8.8	7.9
ERA1	35.4	43.3	44.3	40.4	7.2	8.3	8.5	7.7
NCEP20C	18.8	22.1	21.7	22.2	5.0	6.2	5.3	5.5
ERA20C	27.1	36.8	39.1	35.5	5.4	7.4	7.0	6.7

3.3 OTHER CLIMATOLOGICAL FEATURES

Figure 7 shows the regions favorable to the genesis of all cyclones in summer and winter; the hatched regions indicate positive (blue) and negative (red) trends for cyclogenesis. The hypothesis test for trends is not applied since cyclogenesis has a lot of spatial variability, so that many zero values appear in the time series affecting the statistical test quality (Pezza et al., 2012; Reboita et al., 2018, 2020).

In general, the latitude belt between 50° and 70° S is the most cyclogenetic region of the SH (Figure 7). However, there are two sectors within this belt with the highest cyclones frequency: one at around 170° E and the other at the east of the Antarctic Peninsula, which was also obtained by Crespo (2019). Only NCEP20C (Figure 7f, l) shows a difference in this characteristic, that is, more cyclones to the west of the Peninsula than to the east. ECMWF reanalyses, with emphasis on ERA20C, reveal that there is a predominance of a negative trend in the cyclones frequency between 40° and 55° S, and a positive one in higher latitudes, which is a pattern similar to that obtained in climate projections (Reboita et al., 2018, 2020). NCEP20C shows a negative trend around 60° S and in southern South America, and a positive trend in higher latitudes in both seasons. Despite this difference, NCEP20C also indicates an increase of cyclones frequency at higher latitudes in more recent years.

The sector to the east of the continents (at about 30° S) is also favorable to cyclogenesis and with a higher frequency of systems in winter, in agreement with Reboita et al. (2018, 2020). In South America, this latitude is close to the extreme south of Brazil and Uruguay and corresponds to the cyclogenetic region called RG2 by Reboita et al. (2010) and sometimes denominated by Uruguay (Crespo et al., 2020b). In RG2, there is a positive trend in the cyclones frequency in the NCEP20C reanalysis but, in the other reanalysis is found a gradient of trend with positive trend near Uruguay and negative one in the

neighbourhood. The positive trend highlighted in RG2 is also shown by Reboita et al. (2015). The east coast of South America has two other cyclogenetic regions: the southeast/south coast of Brazil (RG1) and the southeast/south coast of Argentina (RG3). Differently than RG2, in these regions the frequency of cyclones is higher in summer (Figure 7). Moreover, the cyclones in RG1 practically disappear in winter. In summer, the NCEP1 and NCEP2 reanalyses show the well-defined RG1 and RG2 (with two separated cores, Figures 7a-b), and the other reanalyses show a single elongated nucleus connecting these two regions.

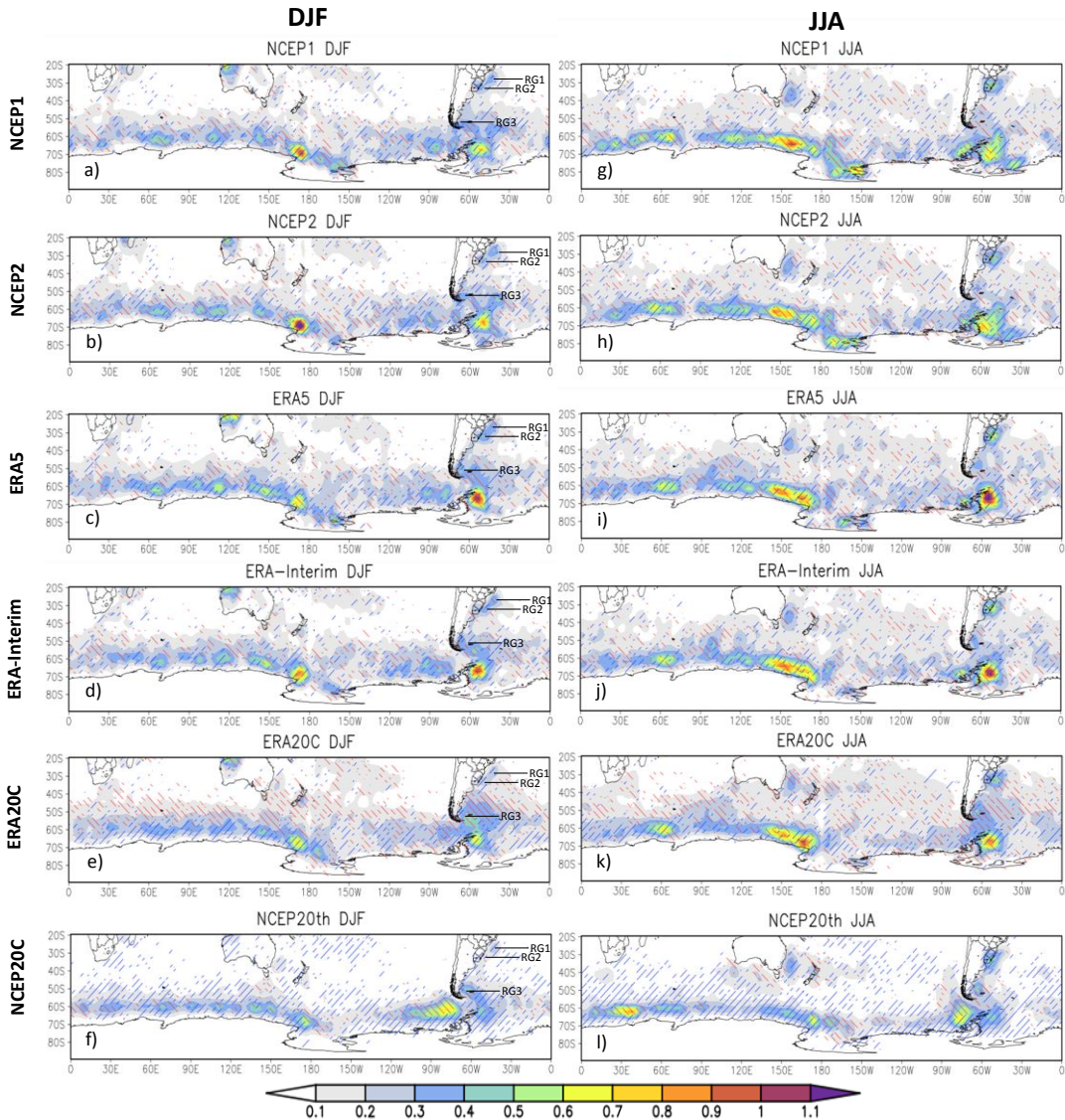


Figure 7 - Seasonal average (colors) of the initial position density (cyclogenesis) of all cyclones identified by the algorithm in summer (left column) and winter (right column) in the different reanalyses. The unit is 10^{-5} km^{-2} . The hatched regions represent positive (blue) and negative (red) trends. In the left column is identified the three cyclogenetic regions on the east coast of South America (RG1, RG2 and RG3).

Reboita et al. (2012) present the physical mechanisms associated with the three cyclogenetic regions on the east coast of South America. Briefly, cyclogenesis in RG1 are more associated with thermodynamic processes, while in RG3 the main forcing are baroclinic and cyclone regeneration processes (cyclonic vorticity is gained by the air column of the flow that crosses the Andes, in latitudes at about 45°S; Hoskins and Hodges, 2005). In RG2, cyclogenesis is favored by a) waves at middle levels of the atmosphere traveling from the Pacific towards the Atlantic, b) the transport of heat and moisture carried out by the low-level jet east of the Andes, c) divergence in mid-upper levels associated with the semi-stationary trough due to the Andean topography and d) the horizontal surface temperature gradients (Gan and Rao, 1991; Vera et al., 2002; Reboita et al., 2012).

In general, the trend of cyclogenesis frequency indicates negative values in both summer and winter in RG3, while in RG1 the signal varies: NCEP and ERA20C reanalyses show a positive trend, and ERA5 and ERAI-Interim show a negative trend near the southeastern coast of Brazil and a positive one towards the south of RG1.

Figure 8 shows the average path density of all cyclones identified in the SH in summer and winter, representing the seasons with the lowest and highest frequency of systems, respectively. The common feature in all reanalyses (Figure 8) is that the cyclone trajectory is more concentrated in a belt around Antarctica in summer, while it expands to the subtropics in winter, a fact associated with the north-south displacement of the most intense horizontal gradient of air temperature (baroclinic zone). In the SH, the baroclinic zone migrates northward (southward) in winter (summer), contributing to the occurrence of extratropical cyclones further away (nearby) from Antarctica. This seasonal feature is evident in Figures 8 and 9, where in summer the meridional gradients of atmospheric pressure (indicated by the marked variation of colors) are concentrated over 45°S and more expanded/displaced to the north in winter.

In winter (Figure 8g-l), a belt of high cyclone density is also evident, extending from southeastern Australia to southern South America. In addition, there is an intense core of systems density in the vicinity of New Zealand. The east coast of South America also has an intense system activity in both seasons. Another fact that stands out in Figure 8 is that, in both summer and winter, the cyclone belt around Antarctica weakens between the Antarctic Peninsula and the southern part of the South Atlantic. This may be a response to the peculiar geography of both South America, which is more extended to the south than the African and Australian continents, and the projection of the Antarctic Peninsula towards lower latitudes. The comparison of the six reanalyses in Figure 8 shows that the spatial pattern of the cyclone path density is similar between them, except for NCEP20C, which shows lower cyclone density (Figures 8f, l).

Regarding the central pressure of cyclones (Figure 9), winter shows greater contrasts in pressure values than summer. During winter, the systems have lower (higher) pressure in the vicinity of Antarctica (subtropical region). In summer, on the other hand, there is less contrast between the high latitudes and the subtropics. Although there are differences in the central pressure averages between the reanalyses, the spatial pattern is similar in all of them.

When it comes to the centenary reanalyses, NCEP20C shows a higher average pressure than ERA20C, which was already indicated in Figure 3.

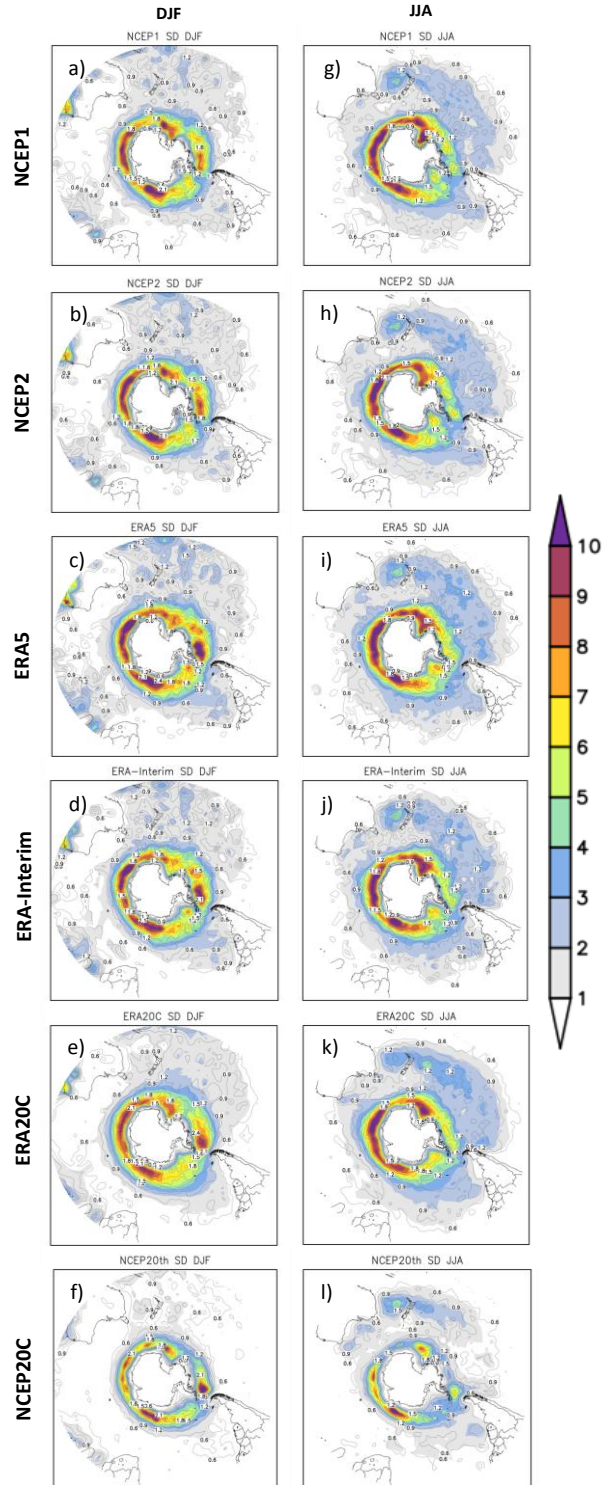


Figure 8 - Seasonal average (colors) and standard deviation (lines) of the trajectory density of all cyclones identified in summer (left column) and winter (right column) in the different reanalyses. The figure unit is (10^{-3} cyclones degrees lat⁻²).

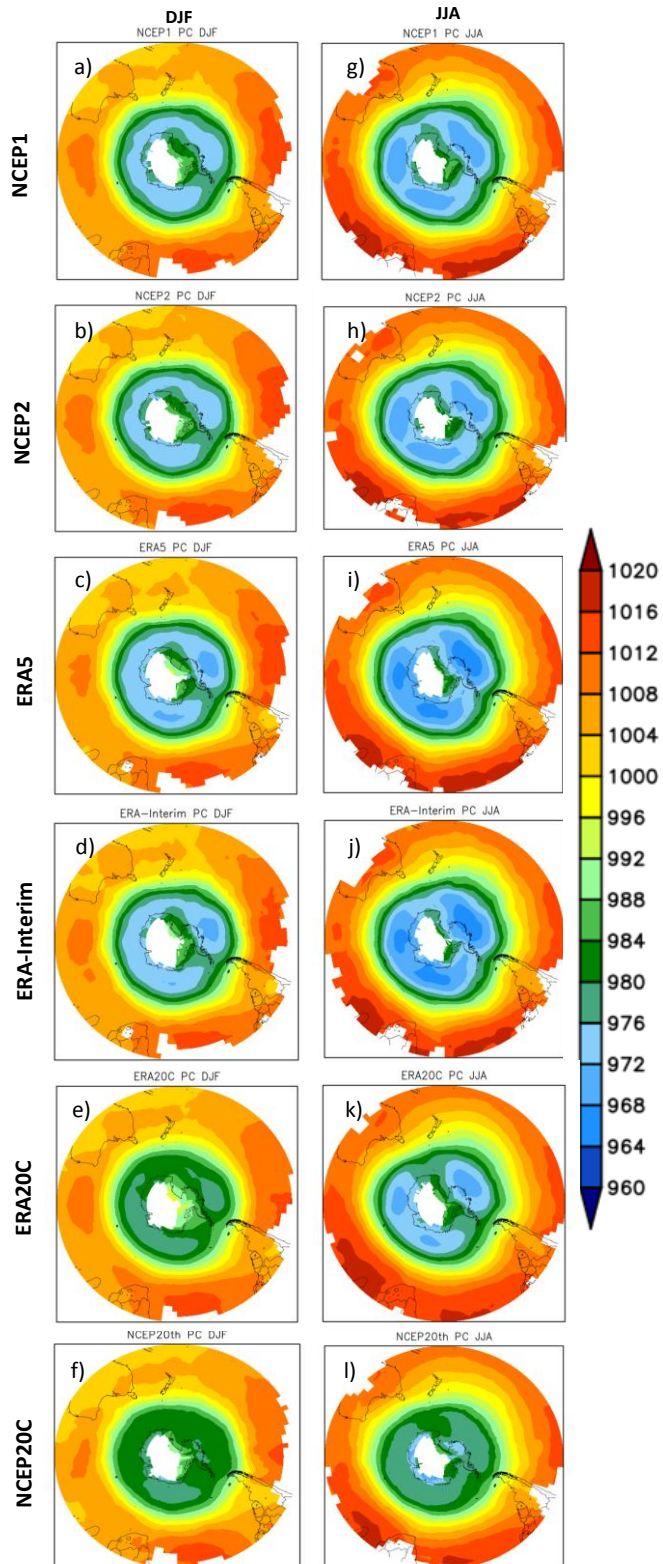


Figure 9 - Seasonal average (colors) of the central pressure (hPa) of all cyclones identified in summer (left column) and winter (right column) in the different reanalyses.

4. CONCLUSIONS

This study compared the cyclone climatology in the Southern Hemisphere in six reanalyses: two centenaries (1900-2018) and four covering a more recent period (1980-2010). The analyses focused on all cyclones identified by the algorithm and on the set of intense systems, i.e., the ones that reach a central pressure lower than or equal to 980 hPa at some point in their lifecycle. In this work, cyclones were identified through MSLP.

Among the main results of the study, we consider:

- 1) There is a big difference in the frequency of cyclones detected in the centennial reanalyses, mainly in the period before 1970. In NCEP20C, the number of cyclones is higher with the increase of the surface data assimilated in the reanalysis. However, this does not occur in ERA20C. We suggest that the near-surface wind over the ocean assimilated in the ERA20C contributes to the better representation of the cyclones and the more homogeneous pattern in the cyclones frequency along the time;
- 2) The current reanalyses obtained using models with a higher horizontal resolution (ERA-Interim and ERA5) show a greater number of cyclones;
- 3) For the Southern Hemisphere and South Atlantic Ocean:
 1. Considering all cyclones from the centennial reanalyses, NCEP20C shows an accentuated and significant positive trend while ERA20C is more homogeneous and with a significant negative trend in the cyclones frequency;
 2. Considering the intense systems, both centennial reanalyses indicate a positive and statistically significant trend in the cyclones frequency in the period 1900-2010;
 3. Considering all cyclones from the recent reanalyses, there is a positive trend over the SH while ECMWF reanalyses (ERA-Interim and ERA5) indicate a negative trend in the cyclones frequency over the South Atlantic between 1980-2018;
 4. Considering the intense systems, the recent reanalyses show a positive trend for systems in the period (1980-2018), but only those from NCEP have a statistical significance over the South Atlantic Ocean;
- 4) On the seasonality of extratropical cyclones, when all cyclones are considered and only those with $P \leq 980$ hPa in the SH, there is a higher (lower) occurrence in the winter (summer) months. When the analysis is restricted to the South Atlantic, the highest cyclones frequency occurs similarly in autumn and winter for all and intense cyclones;
- 5) The latitude belt between 50° and 70°S is the most cyclogenetic region in the SH. At latitudes around 30°S, the sector to the east of the continents is also a favorable region for cyclogenesis;
- 6) The centenary reanalyses indicate a predominance of negative (positive) trend in the cyclones frequency in mid (higher) latitudes, in agreement with climate change studies;
- 7) The east coast of South America has three cyclogenetic regions, where the south/southeastern coast of Brazil (RG1) and the south/southeast of Argentina

(RG3) regions have a higher cyclones frequency in summer, and the southern coast of Brazil and Uruguay (RG2) region has a higher cyclones frequency in winter;

8) In RG1, the NCEP reanalyses and ERA20C show a positive trend in the frequency of cyclones, while ERA5 and ERAI show a negative trend; in RG2, in general, there is a positive trend in the cyclones frequency in the summer (winter); in RG3, the reanalyses indicate negative trends both in summer and winter.

9) No correlation was found between the annual series of cyclone frequency anomalies and PDO, while there is a negative correlation with AMO.

Finally, besides not being possible to state which is the most realistic reanalysis due to the lack of a database from only observations to validate them, most of the climatological features of the cyclones in the different reanalyses are in agreement, which provides reliability for understanding cyclones in the SH.

5. ACKNOWLEDGMENTS

The authors would like to thank CAPES, financial code 001, CNPq, FAPEMIG and PETROBRAS (process 2017/00671-3) for the financial assistance, the University of Melbourne for the algorithm used in the study, and the NCEP and ECMWF for the reanalysis data.

6. REFERENCES

- ALLEN, J. T.; PEZZA, A. B.; BLACK, M. T. Explosive cyclogenesis: A global climatology comparing multiple reanalyses. *Journal of Climate*, 23(24): 6468-6484, 2010.
- BEFORT, D. J.; WILD, S.; KRUSCHKE, T.; ULBRICH, U.; LECKEBUSCH, G. C. Different long-term trends of extra-tropical cyclones and windstorms in ERA-20C and NOAA-20CR reanalyses. *Atmospheric Science Letters*, 17(11): 586-595, 2016.
- BERRISFORD, P.; DEE, D.; POLI, P.; *et al.* The ERA-Interim archive, version 2.0. *ERA Report Series*, 2011. Available in <https://www.ecmwf.int/en/elibrary/8174-era-interim-archive-version-20>
- BLOOMFIELD, H. C.; SHAFFREY, L. C.; HODGES, K. I.; VIDALE, P. L. A critical assessment of the long term changes in the wintertime surface Arctic Oscillation and Northern Hemisphere storminess in the ERA20C reanalysis. *Environmental Research Letters*, 13(9): p. 94004., 2018. doi: <https://doi.org/10.1088/1748-9326/aad5c5>
- CELEMÍN, A. H. *Meteorología Práctica*. Edición del Autor, Mar del Plata, República Argentina, 313 pp, 1984.
- CHANG, E. K.; YAU, A. M. Northern Hemisphere winter storm track trends since 1959 derived from multiple reanalysis datasets. *Climate Dynamics*, 47(5-6): 1435-1454, 2016.

COMPO, G. P.; WHITAKER, J. S.; SARDESHMUKH, P. D.; *et al.* The twentieth century reanalysis project. *Quarterly Journal of the Royal Meteorological Society*, 137(654): 1-28, 2011.

COPERNICUS CLIMATE CHANGE SERVICE (C3S). *ERA5: Fifth generation of ECMWF atmospheric reanalyses of the global climate*, 2017.

CRESPO, N. M. A potential vorticity perspective on cyclones over South America. Tese de Doutorado em Meteorologia, IAG/USP, 104p., 2019. DOI:10.11606/T.14.2019.tde-17122019-154313.

CRESPO, N. M.; DA ROCHA, R. P.; DE JESUS, E. M. Cyclone density and characteristics in different reanalyses dataset over South America. *EGU General Assembly*, 2020a, <https://doi.org/10.5194/egusphere-egu2020-11316>.

CRESPO, N. M.; DA ROCHA, R. P.; SPRENGER, M.; WERNLI, H. A potential vorticity perspective on cyclogenesis over centre-eastern South America. *International Journal of Climatology*, 1-16, 2020b. <https://doi.org/10.1002/joc.6644>.

DE JESUS, E.; DA ROCHA, R. P.; CRESPO, N. M.; REBOITA, M. S.; GOZZO, L. F. Multi-model climate projections of the main cyclogenesis hot-spots and associated winds in South America eastern coast. *Climate Dynamics*, 2020. <https://doi.org/10.1007/s00382-020-05490-1>

ENFIELD, D. B.; MESTAS-NUÑEZ, A. M.; TRIMBLE, P. J. The Atlantic multidecadal oscillation and its relation to rainfall and river flows in the continental U.S. *Geophysical Research Letters*, 28(10): 2077-2080, 2001.

GAN, M. A.; RAO, V. B. Surface cyclogenesis over South America. *Monthly Weather Review*, 119(5): 1293-1302, 1991.

GRIEGER, J.; LECKEBUSCH, G. C.; RAIBLE, C. C.; RUDEVA, I.; SIMMONDS, I. Subantarctic cyclones identified by 14 tracking methods, and their role for moisture transports into the continent. *Tellus A: Dynamic Meteorology and Oceanography*, 70(1): 1-18, 2018.

HERSBACH, H.; BELL, B.; BERRISFORD, P.; HORÁNYI, A.; MUÑOZ-SABATER, J.; NICOLAS, J. P.; RADU, R.; SCHEPERS, D.; SIMMONS, A.; SOCI, C.; DEE, D. ECMWF Global Reanalysis: goodbye ERA-Interim, hello ERA5. *ECMWF Newsletter*, 159: 17-24, 2019.

HODGES, K. I. Confidence intervals and significance tests for spherical data derived from feature tracking. *Monthly Weather Review*, 136(5): 1758-1777, 2008.

HODGES, K. I.; LEE, R. W.; BENGTTSSON, L. A comparison of extratropical cyclones in recent reanalysis ERA-Interim, NASA MERRA, NCEP CFSR, and JRA-25. *Journal of Climate*, 24(18): 4888-4906, 2011.

HODGES, K.; COBB, A.; VIDALE, P. L. How well are tropical cyclones represented in reanalysis datasets?. *Journal of Climate*, 30: 5243-5264, 2017.

HOSKINS, B. J.; HODGES, K. I. A new perspective on Southern Hemisphere storm tracks. *Journal of Climate*, 18(20): 4108-4129, 2005.

KALNAY, E.; KANAMITSU, M.; KISTLER, R.; *et al.* The NCEP/NCAR 40-year reanalysis project. *Bulletin of the American Meteorological Society*, 77(3): 437-472, 1996.

KANAMITSU, M.; EBISUZAKI, W.; WOOLLEN, J.; YANG, S.-K.; HNILO, J. J.; FIORINO, M.; POTTER., G. L. NCEP/DOE AMIP-II reanalysis (R-2), *Bull. Am. Meteorol. Soc.*, 83: 1631 – 1643, 2002.

KAYANO, M. T.; ROSA, M. B.; RAO, V. B.; ANDREOLI, R. V.; SOUZA, R. A. F. Relations of the Low-Level Extratropical Cyclones in the Southeast Pacific and South Atlantic to the Atlantic Multidecadal Oscillation. *Journal of Climate*, 32: 4167-4178, 2019.

KENDALL, M. G. A new measure of rank correlation. *Biometrika*, 30(1/2): 81-93, 1938.

KODAMA, C.; STEVENS, B.; MAURITSEN, T.; SEIKI, T.; SATOH, M. A New Perspective for Future Precipitation Change from Intense Extratropical Cyclones. *Geophysical Research Letters*, 46(21): 12435-12444, 2019.

KUNKEL, K. E.; EASTERLING, D. R.; KRISTOVICH, D. A.; GLEASON, B.; STOECKER, L.; SMITH, R. Meteorological causes of the secular variations in observed extreme precipitation events for the conterminous United States. *Journal of Hydrometeorology*, 13(3): 1131-1141, 2012.

KRUSCHKE, T.; RUST, H. W.; KADOW, C.; LECKEBUSCH, G. C.; ULBRICH, U. Evaluating decadal predictions of northern hemispheric cyclone frequencies. *Tellus A: Dynamic Meteorology and Oceanography*, 66(1): p.22830, 2014.

LECKEBUSCH, G. C.; ULBRICH, U. On the relationship between cyclones and extreme windstorm events over Europe under climate change. *Global and Planetary Change*, 44(1-4): 181-193, 2004.

LECKEBUSCH, G. C.; KOFFI, B.; ULBRICH, U.; PINTO, J. G.; SPANGEHL, T.; ZACHARIAS, S. Analysis of frequency and intensity of European winter storm events from a multi-model perspective, at synoptic and regional scales. *Climate Research*, 31(1): 59-74, 2006.

LEONARD, S. R.; TURNER, J.; VAN DER WAL, A. An assessment of three automatic depression tracking schemes. *Meteorological Applications*, 6(2): 173-183, 1999.

LIM, E. P.; SIMMONDS, I. Southern Hemisphere winter extratropical cyclone characteristics and vertical organization observed with the ERA-40 data in 1979–2001. *Journal of Climate*, 20(11): 2675-2690, 2007.

MANTUA, N. J.; HARE, S. R.; ZHANG, Y.; WALLACE, J. M.; FRANCIS, R. C. A Pacific interdecadal climate oscillation with impacts on salmon production. *Bulletin of the American Meteorological Society*, 78(6): 1069-1080, 1997.

MURRAY, R. J.; SIMMONDS, I. A numerical scheme for tracking cyclone centres from digital data. Part I: Development and operation of the scheme. *Australian Meteorological Magazine*, 39(3): 155-166, 1991a.

MURRAY, R. J.; SIMMONDS, I. A numerical scheme for tracking cyclone centres from digital data. Part II: application to January and July general circulation model simulations. *Australian Meteorological Magazine*, 39(3): 167-180, 1991b.

NEU, U.; AKPEROV, M.; BELLENBAUM, N., *et al.* MILAST: A Community Effort to Intercompare Extratropical Cyclone Detection and Tracking Algorithms. *Bulletin of the American Meteorological Society*, 94 (4): 529-547, 2013.

PEZZA, A. B.; AMBRIZZI, T. Variability of Southern Hemisphere cyclone and anticyclone behavior: Further analysis. *Journal of Climate*, 16(7): 1075-1083, 2003.

PEZZA, A. B.; RASHID, H. A.; SIMMONDS, I. Climate links and recent extremes in Antarctic sea ice, high-latitude cyclones, Southern Annular Mode and ENSO. *Climate Dynamics*, 38(1-2): 57-73, 2012.

PINTO, J. G.; SPANGEHL, T.; ULBRICH, U.; SPETH, P. Sensitivities of a cyclone detection and tracking algorithm: individual tracks and climatology. *Meteorologische Zeitschrift*, 14(6): 823-838, 2005.

POLI, P.; HERBACH, H.; DEE, D. P.; *et al.* ERA-20C: An atmospheric reanalysis of the twentieth century. *Journal of Climate*, 29(11): 4083-4097, 2016.

REBOITA, M. S. *Ciclones extratropicais sobre o Atlântico Sul: Simulação climática e experimentos de sensibilidade* (Tese de doutorado), Universidade de São Paulo (IAG/USP), 2008.

REBOITA, M. S.; DA ROCHA, R. P.; AMBRIZZI, T.; SUGAHARA, S. (2010). South Atlantic Ocean cyclogenesis climatology simulated by regional climate model (RegCM3). *Climate Dynamics*, 35(7-8): 1331-1347, 2010.

REBOITA, M. S.; DA ROCHA, R. P.; AMBRIZZI, T. Dynamic and Climatological Features of Cyclonic Developments over Southwestern South Atlantic Ocean, In: Veress, B.; Szigethy, J. (Org.). *Horizons in Earth Science Research*, 6: 135-160, 2012.

REBOITA, M. S.; DA ROCHA, R. P.; AMBRIZZI, T.; GOUVEIA, C. D. Trend and teleconnection patterns in the climatology of extratropical cyclones over the Southern Hemisphere. *Climate Dynamics*, 45(7-8): 1929-1944, 2015.

REBOITA, M. S.; GAN, M. A.; DA ROCHA, R. P.; CUSTÓDIO, I. S. Ciclones em Superfície nas Latitudes Austrais: Parte I-Revisão Bibliográfica. *Revista Brasileira de Meteorologia*, 32(2): 171-186, 2017.

REBOITA, M. S.; DA ROCHA, R. P.; DE SOUZA, M. R.; LLOPART, M. Extratropical cyclones over the southwestern South Atlantic Ocean: HadGEM2-ES and RegCM4 projections. *International Journal of Climatology*, 38(6): 2866-2879, 2018.

REBOITA, M. S.; REALE, M.; DA ROCHA, R. P.; GIORGI, F.; GIULIANI, G.; COPPOLA, E.; NINO, R. B. L.; LLOPART, M., TORRES, J. A.; CAVAZOS, T. Future Changes in the Wintertime Cyclonic Activity over the CORDEX-CORE Southern Hemisphere domains in a Multi-Model Approach. *Climate Dynamics*, doi: 10.1007/s00382-020-05317-z, 2020.

SIMMONDS, I.; BI, D.; HOPE, P. Atmospheric water vapor flux and its association with rainfall over China in summer. *Journal of Climate*, 12(5): 1353-1367, 1999.

SIMMONDS, I. R.J.; MURRAY, R.M. A refinement of cyclone tracking methods with data from FROST. *Australian Meteorological Magazine* 28: 617-622, 1999.

SIMMONDS, I.; KEAY, K. Mean Southern Hemisphere extratropical cyclone behavior in the 40-year NCEP–NCAR reanalysis. *Journal of Climate*, 13(5): 873-885, 2000.

SIMMONDS, I.; KEAY, K.; LIM, E. P. Synoptic activity in the seas around Antarctica. *Monthly Weather Review*, 131(2): 272-288, 2003.

SINCLAIR, M. R. An objective cyclone climatology for the Southern Hemisphere. *Monthly Weather Review*, 122(10): 2239-2256, 1994.

TILININA, N.; GULEV, S. K.; RUDEVA, I.; KOLTERMANN, P. Comparing cyclone life cycle characteristics and their interannual variability in different reanalyses. *Journal of Climate*, 26(17): 6419-6438, 2013.

TILININA, N.; GULEV, S. K.; BROMWICH, D. H. New view of Arctic cyclone activity from the Arctic system reanalysis. *Geophysical Research Letters*, 41(5): 1766-1772, 2014.

VERA, C. S.; VIGLIAROLO, P. K.; BERBERY, E. H. Cold Season Synoptic-Scale Waves over Subtropical South America. *Monthly Weather Review*, 130: 684-699, 2002.

VESSEY, A. F.; HODGES, K. I.; SHAFFREY, L. C. *et al.* An inter-comparison of Arctic synoptic scale storms between four global reanalysis datasets. *Climate Dynamics*, 54: 2777–2795, 2020.

WANG, X. L.; FENG, Y.; COMPO, G. P.; SWAIL, V. R.; ZWIERS, F. W.; ALLAN, R. J.; SARDESHMUKH, P. D. Trends and low frequency variability of extra-tropical cyclone activity in the ensemble of twentieth century reanalysis. *Climate Dynamics*, 40(11-12): 2775-2800, 2013.

WANG, X. L.; FENG, Y.; CHAN, R.; ISAAC, V. Inter-comparison of extra-tropical cyclone activity in nine reanalysis datasets. *Atmospheric Research*, 181: 133-153, 2016.

WICKSTRÖM, S.; JONASSEN, M. O.; VIHMA, T.; UOTILA, P. Trends in cyclones in the high-latitude North Atlantic during 1979–2016. *Quarterly Journal of the Royal Meteorological Society*, 2019.

ZAHN, M.; AKPEROV, M.; RINKE, A.; FESER, F.; MOKHOV, I. I. Trends of cyclone characteristics in the Arctic and their patterns from different reanalysis data. *Journal of Geophysical Research: Atmospheres*, 123(5): 2737-2751, 2018